



Distinct domains of the $\beta 1$ -subunit cytosolic N terminus control surface expression and functional properties of large-conductance calcium-activated potassium (BK) channels

Received for publication, November 24, 2016, and in revised form, March 17, 2017. Published, Papers in Press, April 3, 2017, DOI 10.1074/jbc.M116.769505

Lie Chen^{‡§}, Danlei Bi^{†¶}, Zen Huat Lu^{§||}, Heather McClafferty[‡], and  Michael J. Shipston^{‡#1}

From the [‡]Centre for Integrative Physiology, College of Medicine and Veterinary Medicine, University of Edinburgh, Edinburgh EH8 9XD, Scotland, United Kingdom, [§]PAPRSB Institute of Health Sciences, Universiti Brunei Darussalam, Jalan Tungku Link BE1410, Brunei Darussalam, [¶]Neurodegenerative Disease Research Center, School of Life Sciences, University of Science and Technology of China, Hefei 230026, China, and ^{||}Division of Genetics and Genomics, The Roslin Institute, University of Edinburgh, Edinburgh EH25 9RG, Scotland, United Kingdom

Edited by F. Anne Stephenson

The properties and function of large-conductance calcium- and voltage-activated potassium (BK) channels are modified by the tissue-specific expression of regulatory $\beta 1$ -subunits. Although the short cytosolic N-terminal domain of the $\beta 1$ -subunit is important for controlling both BK channel trafficking and function, whether the same, or different, regions of the N terminus control these distinct processes remains unknown. Here we demonstrate that the first six N-terminal residues including Lys-3, Lys-4, and Leu-5 are critical for controlling functional regulation, but not trafficking, of BK channels. This membrane-distal region has features of an amphipathic helix that is predicted to control the orientation of the first transmembrane-spanning domain (TM1) of the $\beta 1$ -subunit. In contrast, a membrane-proximal leucine residue (Leu-17) controls trafficking without affecting functional coupling, an effect that is in part dependent on controlling efficient endoplasmic reticulum exit of the pore-forming α -subunit. Thus cell surface trafficking and functional coupling with BK channels are controlled by distinct domains of the $\beta 1$ -subunit N terminus.

Large-conductance calcium- and voltage-activated potassium channels are ubiquitously expressed and regulate a diverse array of physiological processes (1). This is associated with a wide functional diversity with the functional properties of BK² channels being adapted to the physiological requirements of specific cell types. Disruption of BK channel function in human and animals is associated with a wide range of pathologies ranging from hypertension, autism, asthma, cancer, diabetes, and obesity to other disorders of the vascular, nervous, endocrine, and other systems.

The pore-forming α -subunit is encoded by a single gene (*KCNMA1*). However, BK channels in native tissues show distinct properties (1–3). This functional diversity is generated by multiple mechanisms including alternative splicing and post-translational modification of the α -subunit (3) as well as through assembly with a range of transmembrane accessory β - and γ -subunits (4, 5).

Regulatory $\beta 1$ -subunits, which have a distinct tissue distribution and play an important role in vascular and other smooth muscle, exert diverse functional effects on the α -subunit. Indeed, genetic deletion of $\beta 1$ -subunits in mice leads to hypertension, and mutations in the $\beta 1$ -subunit are associated with hypertension and asthma. $\beta 1$ -subunits consist of two transmembrane-spanning domains (TM1 and TM2) with short intracellular N- and C-terminal domains and a large extracellular loop coupling TM1 to TM2. $\beta 1$ -subunits control multiple aspects of BK channel function. The subunits control BK channel cell surface expression that is dependent on domains within both α - and $\beta 1$ -subunits (6–8). Importantly, $\beta 1$ -subunits also confer functional regulation of BK channel properties (6, 9, 10) including a large hyperpolarizing shift in the conductance-voltage relationship of macroscopic currents as a result of changes in apparent calcium sensitivity, a shift in magnesium sensitivity, and modification of gating through control of voltage sensing and slowing of channel activation and deactivation. Moreover, $\beta 1$ -subunits confer regulation by a diverse array of molecules including hormones, alcohol, fatty acids, and drugs (11).

Although $\beta 1$ -subunits confer such a diversity of modulation of BK channel function, specific domains and residues in the $\beta 1$ -subunit that are important for control are only beginning to emerge. For example, both the N and C termini of the $\beta 1$ -subunit have been implicated in the control of BK channel surface expression as well as the control of functional properties (7, 8, 10, 12–14). However, whether distinct regions of the $\beta 1$ -subunit confer different effects on channel trafficking compared with effects on functional coupling or sensitivity or similar regions control overlapping modes of regulation is poorly understood. Important in this regard is that studies, using both biochemical and biophysical/optical approaches, to investigate how $\beta 1$ -subunits and α -subunits assemble in the membrane are beginning to reveal the importance of the location of both the

This work was supported by a in part by grants from the Wellcome Trust, Diabetes UK, and Medical Research Council (to M. J. S.). The authors declare that they have no conflicts of interest with the contents of this article.

✂ Author's Choice—Final version free via Creative Commons CC-BY license.

¹ To whom correspondence should be addressed. Tel.: 44-131-6503253; E-mail: mike.shipston@ed.ac.uk.

² The abbreviations used are: BK, large-conductance calcium- and voltage-activated potassium; TM, transmembrane-spanning domain; ER, endoplasmic reticulum; G/V, conductance-voltage; myc_c, C-terminal myc; myc_e, extracellular myc; fwd, forward; rev, reverse; ANOVA, analysis of variance; BGH, bovine growth hormone.

transmembrane and intracellular N termini of β 1-subunits in relationship with transmembrane and other domains of the α -subunit (15, 16). Importantly, such studies suggest that the TM1 and TM2 of β 1-subunits as well as the S0 domain of α -subunits have different trajectories through the plasma membrane.

Moreover, studies are beginning to reveal the role of specific amino acid residues in the short (18-amino-acid) N terminus of β 1 in controlling both surface expression and functional coupling. For example, mutation of two basic residues (Lys-3 and Lys-4) largely abolishes gating charge movement in the absence of calcium, suggesting that these residues play a critical role in stabilizing the voltage sensor (10). In addition, mutant cycle analysis has suggested a role for a hydrophobic patch of residues (Leu-5, Val-6, and Met-7) and an electrostatic enhancing site (Glu-13 and Thr-14) that are proposed to mediate interactions of β 1-subunits with different regions of the α -subunit to control magnesium and calcium sensitivity (12). Conversely, deletion of the entire N terminus abolishes functional coupling as well as the reported β 1-subunit-induced enhancement of BK channel surface expression (7, 14), although residues important in the cytosolic N terminus of mammalian β 1-subunits that control BK trafficking are not defined.

Increasing evidence also suggests that distinct regions of the β 1-subunit N terminus may be targets for differential regulation. For example, amino acids in the membrane-proximal region of the N terminus are important for the ability of ω -3 fatty acids to activate the BK channel $\alpha\beta$ 1 complex (17, 18) and have been implicated in the potential beneficial effects of ω -3 fatty acids in blood pressure control. In contrast, somatic cancer mutations have been reported that cluster around the basic and hydrophobic residues in the more distal region of the N terminus (19, 20) with changes in BK channel activity linked to cancer cell proliferation and migration (21–23).

In this study, we sought to address whether the surface trafficking effects mediated by the β 1-subunit N terminus required similar or distinct regions of the N terminus as those that control functional regulation. To address this issue, we exploited an integrated mutagenesis and deletion strategy coupled with surface expression and functional macroscopic current analysis. Here we demonstrate that distinct N-terminal residues of the β 1-subunit control functional coupling to α -subunits and control α -subunit surface expression, respectively.

Results

Membrane-proximal domain of β 1-subunit N terminus is required for enhanced trafficking of BK α -subunit ZERO variant

To address the role of the intracellular N terminus of the β 1-subunit in enhancing the cell surface expression of the pore-forming α -subunit, we used a cell surface imaging assay to investigate the co-expression of β 1-subunit deletion and site-directed mutants with a C-terminal myc (-myc) tag (β 1-myc_c) and the BK channel α -subunit ZERO variant with an extracellular N-terminal FLAG (FLAG-) tag.

By analyzing the cell surface FLAG- signal levels under non-permeabilized conditions (expressed as a percentage of total

α -subunit expression following membrane permeabilization) in anti-myc-positive HEK293 cells, we found that wild-type β 1-subunits significantly enhanced the cell membrane surface expression of ZERO by more than 2-fold ($232.3 \pm 22.7\%$, $n = 7$; Fig. 1, A–C) in comparison with that of ZERO alone ($100 \pm 7.8\%$, $n = 8$). Deletion of the predicted N terminus of the β 1-subunit (β 1- Δ 17-myc_c mutant with N-terminal amino acids 2–18 deleted) resulted in no significant enhancement of ZERO cell surface expression (Fig. 1, A–C). The loss of enhancement, however, was not the result of poor expression of ZERO. In fact, in transfected cells, the N terminus-deleted mutant β 1- Δ 17-myc_c displayed a similar robust expression level as that of wild-type β 1-myc_c, suggesting that changes in protein expression do not underlie the deficit in promoting surface expression of the ZERO α -subunit. Moreover, the physical interaction of β 1- Δ 17-myc_c and ZERO subunits was not disrupted as FLAG-ZERO and β 1- Δ 17-myc_c could co-immunoprecipitate in pulldown assays (data not shown). We asked whether the inability of the β 1- Δ 17-myc_c deletion mutant to promote cell surface expression of ZERO may be a consequence of the inability of the deletion mutant to traffic to the cell surface alone. To test this, we generated β 1 mutants harboring an additional extracellular myc (myc_e) tag to allow for the quantification of β 1-subunit cell surface expression. Wild-type β 1-myc_{c&e} mutants were efficiently trafficked to the cell surface alone. However, this was reduced to $10.3 \pm 1.2\%$ ($n = 11$) of wild-type levels with the N-terminal deletion mutant β 1- Δ 17-myc_{c&e} (Fig. 2, A and B). Thus, the N terminus of the β 1-subunit is required for both efficient surface expression of the β 1-subunit *per se* and the ability of the β 1-subunit to promote ZERO α -subunit surface expression.

To define the domains of the intracellular N terminus important for the enhanced cell surface expression of ZERO subunits, we first took a deletion strategy to remove increasingly larger distal regions of the intracellular N terminus of the β 1-subunit. Deletion of residues 1–6 or 2–10 (β 1- Δ 6-myc_c and β 1- Δ 9-myc_c constructs) of the β 1-subunit N terminus promoted cell surface expression of ZERO by more than 2-fold and was not distinguishable from wild-type β 1-subunit (Fig. 1, B and C). Deletion of residues 2–14 (β 1- Δ 14-myc_c construct) also significantly promoted cell surface expression by almost 1.8-fold, suggesting that the first 14 amino acids are largely dispensable for promoting cell surface expression of the ZERO subunit.

Lysine 17 is important for β 1-subunit enhancement of ZERO α -subunit surface expression

To refine the N-terminal residues important for enhanced cell surface trafficking of ZERO promoted by the β 1-subunit, we used an alanine substitution-scanning approach of residues immediately preceding residue 14 up to cysteine 18 at the membrane interface. We constructed single or multiple alanine-substituted mutations of C-terminal myc (myc_c)-tagged β 1-subunits β 1-(K10A,R11A)-myc_c, β 1-(R11A,G12A,E13A)-myc_c, β 1-T14A-myc_c, β 1-R15A-myc_c, β 1-L17A-myc_c, and β 1-C18A-myc_c and co-expressed each of them with FLAG-ZERO in HEK293 cells. The alanine-mutated β 1-subunits promoted cell surface expression of ZERO subunits to a similar extent as wild-type β 1-subunits except for β 1-L17A-myc_c

β 1-subunit N terminus controls function of BK channels

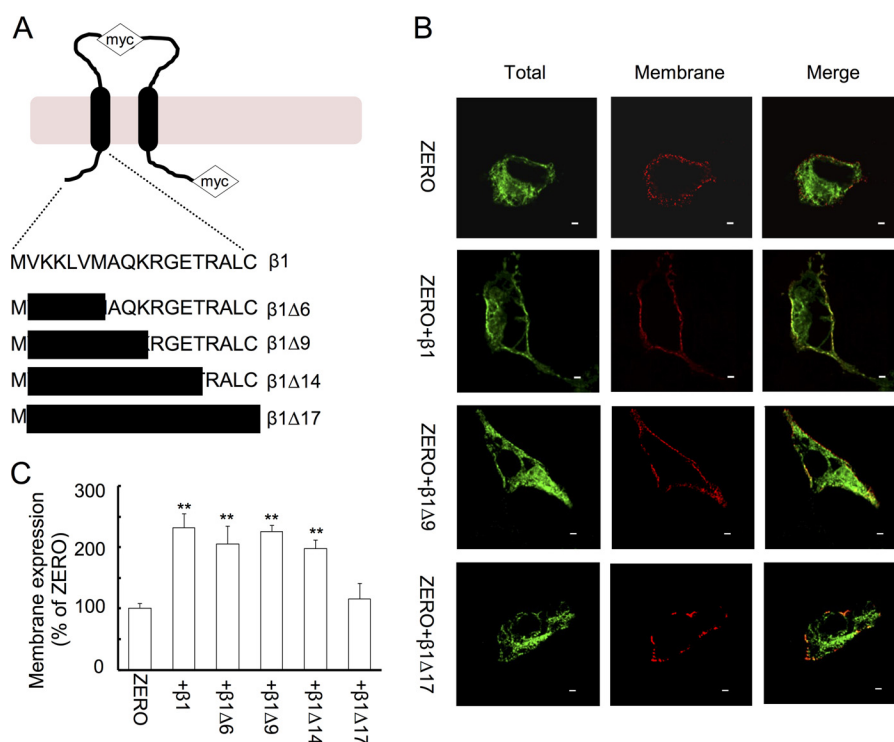


Figure 1. Membrane-proximal residues of β 1-subunit N terminus control surface expression and pore-forming α -subunit ZERO variants. *A*, schematic of β 1-subunit topology with residues of N-terminal deletion mutants indicated along with the C-terminal and extracellular myc tags used in these studies. *B*, representative single confocal images of the cell surface (membrane) and intracellular (permeabilized) expression of FLAG-ZERO determined in the presence and absence of wild-type β 1 subunits with a C-terminal myc tag (β 1-myc_c) and respective mutants in HEK293 cells. Scale bars, 2 μ m. *C*, quantification of cell surface membrane expression of FLAG-ZERO with the respective β 1-subunit deletion mutants expressed as a percentage of FLAG-ZERO surface expression alone (100%). Data are means, and error bars represent S.E. ($N > 8$; $n > 50$ /group). **, $p < 0.01$ compared with ZERO alone (ANOVA with Dunnett's post hoc test).

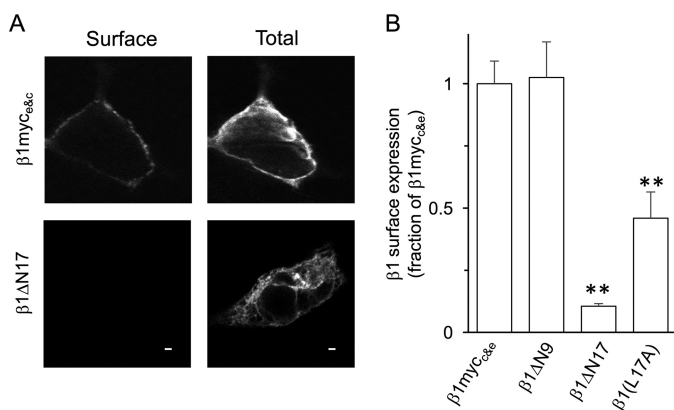


Figure 2. N terminus of β 1-subunit controls surface trafficking of β 1-subunit alone. *A*, representative single confocal images of the cell surface (membrane) and total (permeabilized) expression of wild-type and mutant β 1-subunits with both C-terminal and extracellular myc tags (β 1-myc_{c&e}) in HEK293 cells. Scale bars, 2 μ m. *B*, quantification of cell surface membrane expression of the respective β 1-subunits expressed as a fraction of wild-type (β 1-myc_{c&e}) surface expression alone. Data are means, and error bars represent S.E. ($N > 4$; $n > 30$ /group). **, $p < 0.01$ compared with β 1-myc_{c&e} alone (ANOVA with Dunnett's post hoc test).

(55.7 \pm 5.0%, $n = 9$), which significantly decreased the enhanced membrane expression level of ZERO (Fig. 3A). This result suggests that Leu-17 of β 1-subunits plays an important role in controlling the enhanced membrane trafficking of ZERO.

To understand how Leu-17 may control the β 1-subunit enhancement of ZERO surface expression, we asked whether

the β 1-subunit β 1- Δ 17-myc_c is important for controlling endoplasmic reticulum (ER) exit of ZERO. We co-expressed FLAG-ZERO and wild-type β 1-myc_c or β 1 mutants together with pDsRed-ER, a vector that encodes a fusion protein. After deconvolution of confocal images, ZERO colocalization with the ER in the presence of different β 1-subunits was analyzed (Fig. 3, B and C). Expression of ZERO alone resulted in a Pearson's correlation coefficient of 0.82 ± 0.03 ($n = 8$) for ZERO with ER. This was significantly reduced upon co-expression of wild-type β 1 to 0.53 ± 0.05 ($n = 8$), revealing that β 1-subunits promote ER exit of ZERO. The ER colocalization of ZERO in the presence of the N-terminal truncated β 1-subunit (β 1- Δ 17-myc_c) was not significantly different from ER localization of ZERO in the absence of β 1-subunits (ER colocalization was 0.82 ± 0.02 ; $n = 8$) (Fig. 3, B and C). Co-expression of ZERO with the β 1-L17A subunit resulted in an ER colocalization of ZERO that was intermediate between ER colocalization of ZERO expressed alone and in the presence of wild-type β 1-subunits at 0.65 ± 0.05 ($n = 8$; Fig. 3, B and C). This partial effect of the L17A mutation on ER trapping is in agreement with the incomplete (~50%) suppression of β 1-subunit enhanced BK channel α -subunit surface expression conferred by the L17A mutation compared with complete deletion of the N terminus (compare β 1- Δ 17-myc_c in Fig. 1C with β 1-L17A in Fig. 3A). Thus, although Leu-17 plays an important role in controlling BK channel surface expression and contributes to ER exit of the ZERO α -subunit, additional features conferred by the most membrane-proximal N-terminal residues (*i.e.* after

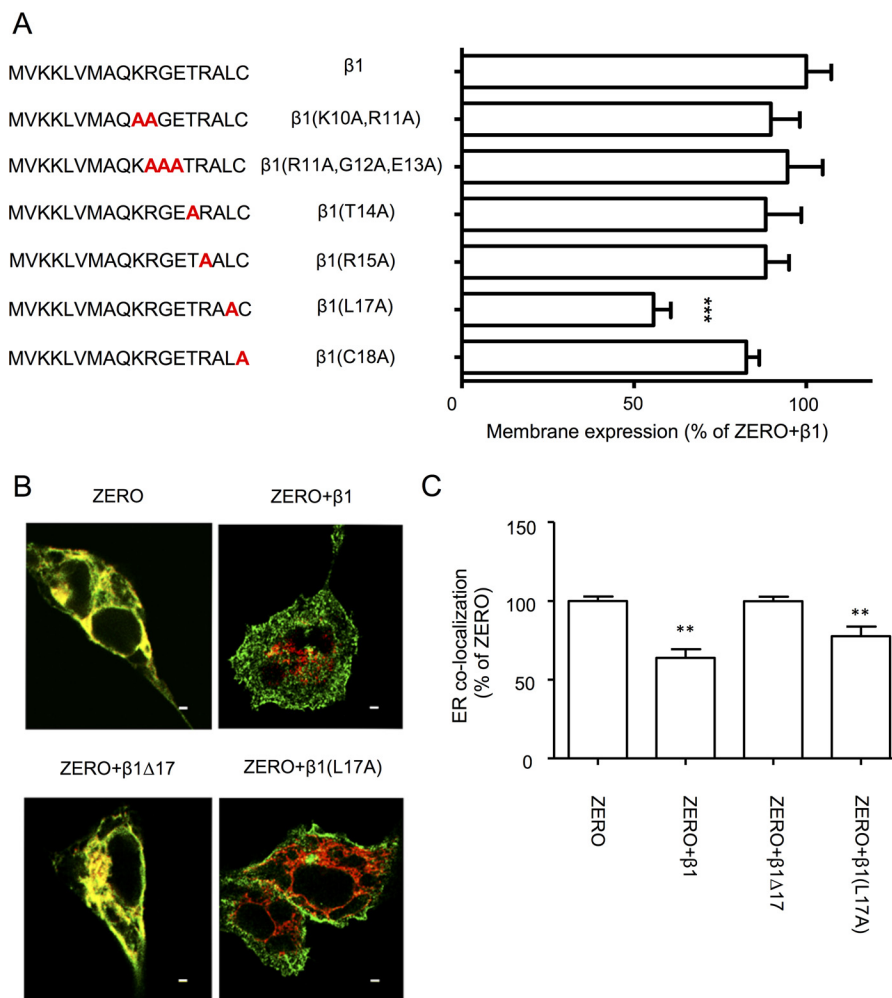


Figure 3. Leu-17 of N-terminal $\beta 1$ -subunit controls surface expression BK α -subunit ZERO variant. A, alanine substitution mutagenesis of membrane-proximal residues in the N terminus of -myc_c-tagged $\beta 1$ -subunits and quantification of the respective cell surface FLAG-ZERO expression in the presence of each mutant. Data are normalized to FLAG-ZERO surface expression in the presence of wild-type $\beta 1$ -myc_c (100%). ***, $p < 0.001$. B, representative single confocal images of FLAG-ZERO (green) co-expressed with wild-type or mutant $\beta 1$ -subunits in HEK293 cells and the endoplasmic reticulum marker (pDsRed-ER) (red) with ER colocalization shown in yellow. Scale bars, 2 μ m. C, bar chart of quantitative ER colocalization of ZERO (expressed as a percentage of the Pearson's correlation coefficient (R value) for ZERO alone (100% = R value of 0.82 \pm 0.03) in the presence of the respective $\beta 1$ -L17A and $\beta 1$ - $\Delta 17$ mutants. Data are means, and error bars represent S.E. ($N > 8$; $n > 50$ /group). **, $p < 0.01$ compared with ZERO alone (ANOVA with Dunnett's post hoc test).

residue 14) are also required for efficient ER exit and surface trafficking.

To examine whether the reduction in ER export in the presence of the $\beta 1$ -subunit N terminus or the L17A mutant is a result of a defect of ER exit of the $\beta 1$ -subunit itself, we performed cell surface expression and ER colocalization using the $\beta 1$ -subunit mutant with an additional extracellular myc tag as above (Fig. 2B). Compared with wild-type $\beta 1$ -subunit alone, surface expression of the $\beta 1$ - $\Delta 17$ -myc_{e&c} and the $\beta 1$ -L17A-my_{e&c} was only 10.3 \pm 1.2 ($n = 4$) and 48.4 \pm 6.7% ($n = 4$), respectively, of wild-type $\beta 1$ -subunit surface expression (Fig. 2B). In addition, co-expression of either $\beta 1$ - $\Delta 17$ -myc_c or $\beta 1$ -L17A-my_c alone with the ER expression vector pDsRed-ER increased ER colocalization of the mutant $\beta 1$ -subunit when compared with the wild-type $\beta 1$ -subunit. The R value of wild-type $\beta 1$ was 0.66 \pm 0.05 ($n = 4$), whereas the values for mutant $\beta 1$ - $\Delta 17$ -myc_{e&c} and $\beta 1$ -L17A-my_{e&c} were 0.85 \pm 0.02 ($n = 4$) and 0.82 \pm 0.02 ($n = 4$), respectively. Thus, at least in part, the reduced cell surface expression of ZERO subunits promoted by

$\beta 1$ -subunits is likely dependent upon the ability of the $\beta 1$ -subunit to exit the ER itself.

Membrane-distal residues of the $\beta 1$ -subunit N terminus determine functional coupling with α -subunits

In accordance with previous data revealing the importance of an intact N terminus of the $\beta 1$ -subunits for functional coupling to α -subunits (13, 14), deletion of the entire N terminus ($\beta 1$ - $\Delta 17$) abolished both the significant left shift of the conductance voltage curve and slowing of activation and deactivation observed across all intracellular free Ca^{2+} concentrations analyzed ranging from 1 to 100 μ M (Fig. 4).

In the presence of 10 μ M intracellular free Ca^{2+} , the $V_{0.5max}$ of ZERO expressed alone was 19.8 \pm 1.2 mV ($n = 33$; Fig. 4, B and C). This was left shifted by ~ 40 mV to -20.5 ± 1.5 mV ($n = 45$) by the wild-type $\beta 1$ -myc_c subunit but not by the mutant $\beta 1$ - $\Delta 17$ -myc_c ($V_{0.5max}$ was 12.2 \pm 1.9 mV; $n = 14$) (Fig. 4, B and C). In control experiments, we observed that the presence of the -myc_c tag attenuated the left shift induced by $\beta 1$ -subunits by

β 1-subunit N terminus controls function of BK channels

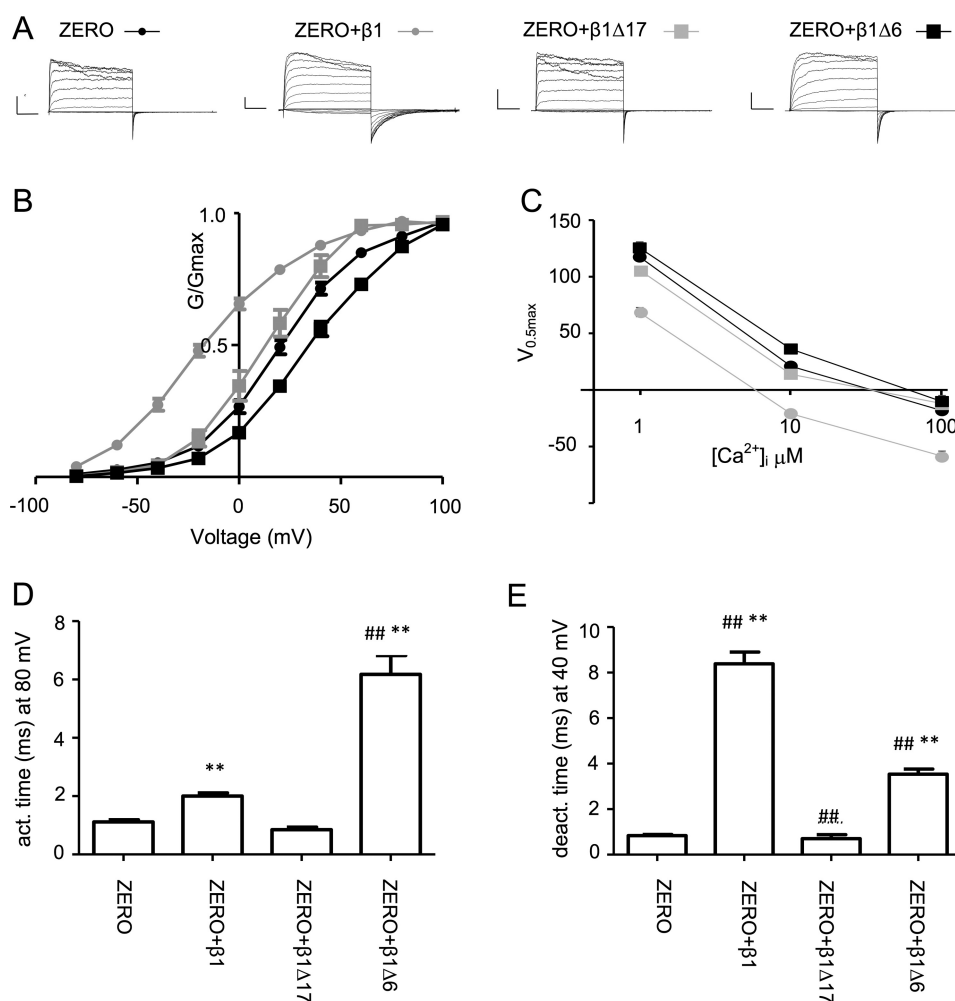


Figure 4. First six residues of β 1-subunit N terminus are essential for functional coupling with α -subunit ZERO variant. A, representative macropatch current recordings from excised inside-out patches from HEK293 cells expressing the ZERO variant and respective β 1-subunit mutants in the presence of 10 μ M intracellular free calcium with voltage protocols as described under "Experimental procedures." B, G/V relationship for constructs as in A with curve fits using the Boltzmann equation (see "Experimental procedures"). C, voltage of half-maximal conductance ($V_{0.5max}$) in the presence of 1, 10, or 100 μ M intracellular free calcium. D and E, activation (*act.*) time constant (D) and deactivation (*deact.*) time constant (E) for the respective ZERO and β 1-subunit combinations in A. Data are means, and error bars represent S.E. ($N > 10$ /group). **, $p < 0.01$ compared with ZERO alone; ##, $p < 0.01$ compared with ZERO + wild-type β 1-myc_c (ANOVA with Dunnett's post hoc test).

17.7 mV. The activation time constants (determined at 80 mV) and deactivation time constants (determined at 40 mV) of ZERO ($n = 33$) were both significantly slowed by wild-type β 1-myc_c ($n = 45$) subunit from 1.12 ± 0.07 and 0.84 ± 0.06 ms to 2.00 ± 0.11 and 8.39 ± 0.52 ms, respectively (Fig. 4, D and E). However, both activation and deactivation time constants (0.85 ± 0.09 and 0.70 ± 0.18 ms, respectively) were not significantly shifted in the presence of β 1- Δ 17-myc_c ($n = 14$; Fig. 4, D and E). These results confirm that the intracellular N terminus of β 1 is essential for its regulation of the electrophysiological properties of BK channels.

To examine whether deletion of the first six residues of the N terminus, which do not affect β 1-subunit-mediated enhancement of ZERO trafficking, would change its functional coupling with α -subunits, we co-expressed the mutant β 1- Δ 6-myc_c subunit with the ZERO variant. In contrast to the left shift mediated by wild-type β 1-subunits, β 1- Δ 6-myc_c induced a small but significant right shift in $V_{0.5max}$ to 35.7 ± 1.6 mV ($n = 14$) when compared with ZERO alone (Fig. 4, B and C). Therefore, the absence of the first six residues of β 1-subunit completely abol-

ished the left shift of the conductance-voltage (G/V) relationship induced by the wild-type β 1. These data reveal that distinct domains of the N terminus control functional coupling and trafficking regulated by β 1-subunits. However, although β 1- Δ 6-myc_c still significantly slowed BK channel activation and deactivation compared with ZERO alone, BK channel activation and deactivation rates in the presence of β 1- Δ 6-myc_c were significantly different compared with those in the presence wild-type β 1-myc_c (Fig. 4, D and E). BK channel activation was slowed to a greater extent with β 1- Δ 6-myc_c compared with wild-type β 1-myc_c, whereas deactivation was faster with β 1- Δ 6-myc_c compared with wild-type β 1-myc_c.

Does the N terminus of the β 1-subunit form an amphipathic α -helix to control functional coupling?

The first six residues of the β 1-subunit include a pair of basic residues (Lys-3 and Lys-4) that are important for gating in the absence of calcium (10), most likely dependent on the interaction of these residues with negative charges. In an attempt to further understand why the first six residues of the N terminus

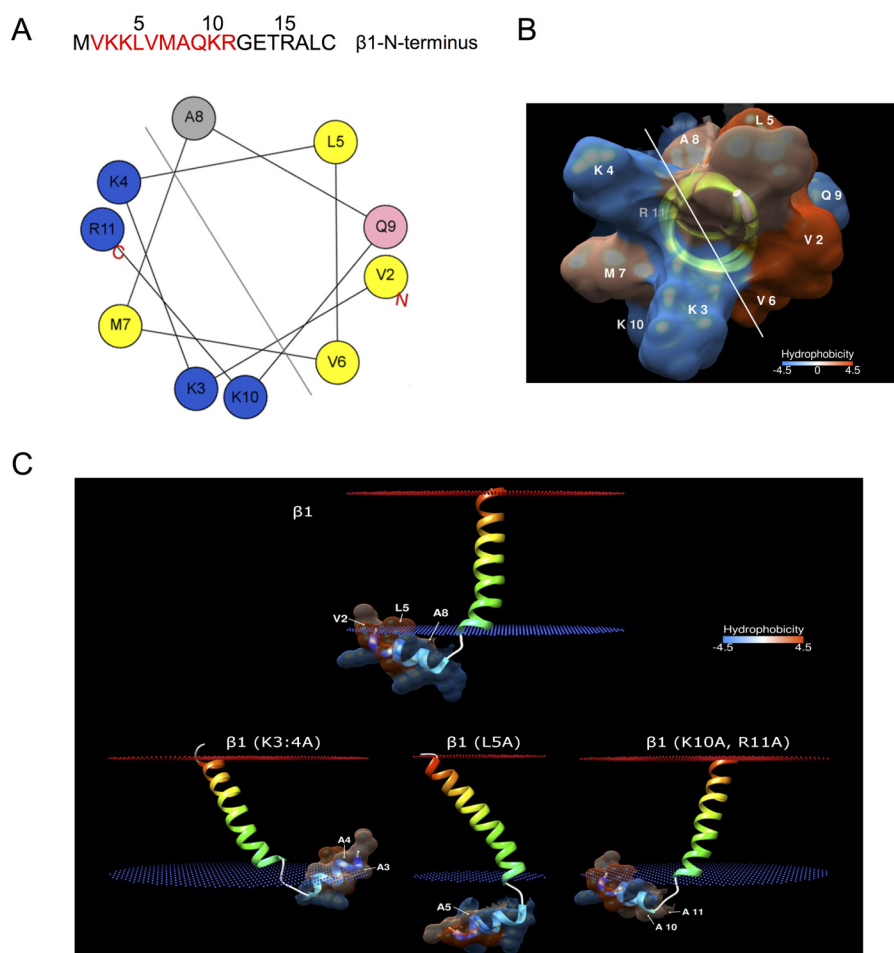


Figure 5. Does the $\beta 1$ -subunit N terminus form an amphipathic helix? A, helical wheel depiction of the N-terminal amphipathic α -helix (residues 2–11). The color code for residues is as follows: yellow, hydrophobic; purple, serine and threonine; blue, basic; red, acidic; pink, asparagine and glutamine; gray, alanine and glycine; green, proline; light blue, histidine. B, hydrophobicity of the amphipathic α -helix represented by a red and blue scale, respectively. C, molecular system of the $\beta 1$ -subunit N terminus and TM1 interaction with a membrane lipid bilayer (blue and red dotted outer and inner membrane, respectively). The hydrophobic Val-2, Leu-5, and Ala-8 on the amphipathic N-terminal helix are anchored onto the membranes. Increased interaction between the N terminus and membrane occurs when charged polar residues are mutated to hydrophobic residues. Leu-5 is predicted to be vital for this interaction.

are important for functional coupling, we analyzed the computationally modeled secondary and tertiary structure of the N terminus and the first transmembrane domain of the $\beta 1$ -subunit embedded within the lipid bilayers of an artificial membrane. Increasing evidence suggests that regions of the $\beta 1$ N terminus are likely to interact with the α -subunit (e.g. see Refs. 15 and 16) and that the orientation of the $\beta 1$ -subunit transmembrane domains is likely to be important for interaction and coupling. Residues 2–11 of the $\beta 1$ -subunit N terminus display the characteristic spatial segregation of hydrophilic and hydrophobic amino acids of an amphipathic α -helix (Fig. 5A). Furthermore, the tertiary structure of the N terminus of $\beta 1$ -subunit, connected through an extended flexible loop with its first transmembrane domain, suggests that the extreme end of the intracellular N-terminal region is likely to fold into three helical turns with opposing hydrophobic and hydrophilic surfaces (Fig. 5B).

When a molecular system consisting of membrane- $\beta 1$ -subunit complex was simulated, the hydrophilic surface formed by the polar residues Lys-3, Lys-4, Lys-10, and Arg-11 of $\beta 1$ -subunit is predicted to be oriented away from the membrane facing the cytoplasm, whereas the hydrophobic surface of residues

Val-2, Leu-5, and Ala-8 serves as a potential membrane anchorage site that supports the association of the intracellular N terminus with the membrane (Fig. 5C). The anchorage is predicted to occur when residues Val-2, Leu-5, and Ala-8 insert themselves into the membrane where their side chains may interact with those of the membrane lipid bilayers. This hydrophobic interaction was markedly affected when the interacting residues were mutated in our modeled molecular systems. For instance, the anchorage was severely disrupted when Leu-5 was mutated to a far less hydrophobic neutral alanine (Fig. 5C), whereas a similar change in V6A (not shown) and K10A,R11A on the cytoplasm-facing hydrophilic surface did not have any significant impact on the hydrophobic interaction between the helix and membrane (Fig. 5C).

However, the helical structure of the K3A,K4A mutant was rotated, and together with other hydrophobic residues they form a much stronger hydrophobic interaction with the membrane. If such a membrane interface (or potential interface with regions of the α -subunit) do indeed exist in the channel complex, the interaction between the amphipathic α -helical N terminus and the membrane may therefore offer a mechanistic insight into the underlying functional coupling between α -sub-

β 1-subunit N terminus controls function of BK channels

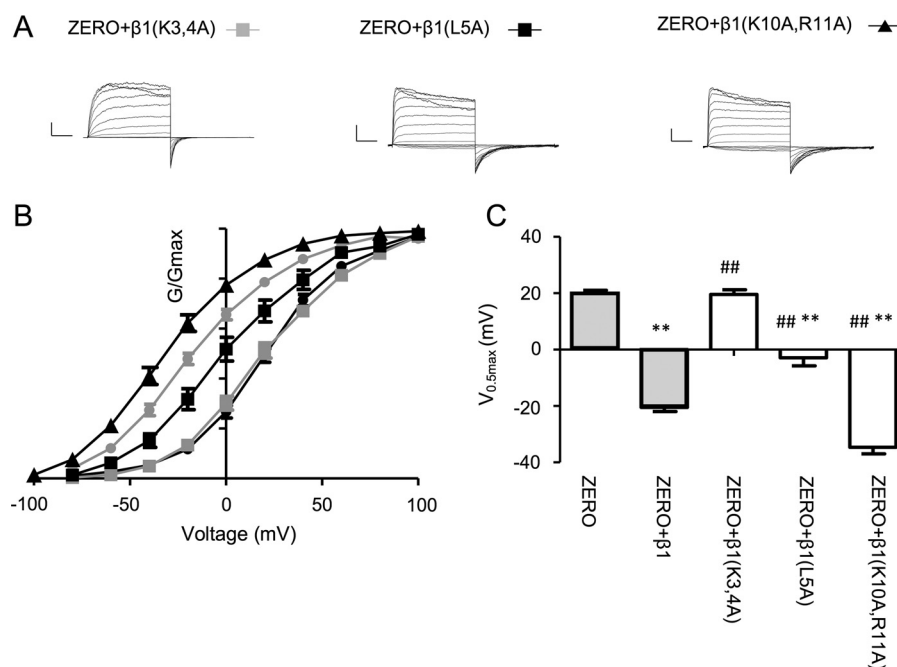


Figure 6. Lys-3, Lys-4, and Leu-5 of β 1-subunit N terminus are important determinants of functional coupling. A, representative macropatch current recordings from excised inside-out patches from HEK293 cells expressing the ZERO variant and respective β 1-subunit mutants in the presence of $10 \mu\text{M}$ intracellular free calcium with voltage protocols as described under "Experimental procedures." B and C, G/V relationship for constructs with curve fits using the Boltzmann equation (see "Experimental procedures") (B) and voltage of half-maximal conductance (C) for the respective ZERO and β 1-subunit combinations in A. The data for ZERO (shaded box) and ZERO with wild-type β 1-subunit (shaded box) are from Fig. 4 and shown for comparison. Data are means, and error bars represent S.E. ($N > 10/\text{group}$). **, $p < 0.01$ compared with ZERO alone; ##, $p < 0.01$ compared with ZERO + wild-type β 1-myc_c (ANOVA with Dunnett's post hoc test).

units and β 1-subunits. Importantly, such a model would predict that mutation of the basic Lys-3 and Lys-4 (as well as hydrophobic Leu-5) but not Lys-10 and Arg-11 residues would control functional coupling and support the functional data above that the first six residues of the N terminus are involved in functional coupling and distinct from those controlling β 1-subunit-mediated enhancement of α -subunit cell surface expression.

To test this model, we examined whether mutating Lys-3 and Lys-4 to alanine (β 1-(K3A,K4A)-myc_c) would result in the loss of functional coupling as predicted and observed in the β 1- Δ 6-myc_c deletion mutant. In the presence of β 1-(K3A,K4A)-myc_c, there was no significant left shift of the G/V relationship of ZERO, resulting in a $V_{0.5max}$ of $19.6 \pm 1.6 \text{ mV}$ ($n = 11$), similar to ZERO alone under these conditions (Fig. 6, A–C). In further support of the model, mutation of the more membrane-proximal basic residues to alanine (K10A,R11A) still significantly left-shifted the G/V relationship of ZERO to a $V_{0.5max}$ of $-31.2 \pm 5.1 \text{ mV}$ ($n = 10$), a value in fact slightly more left-shifted compared with wild-type β 1-myc_c (Fig. 6, B and C). Thus, as predicted by the modeling, the lack of functional regulation by β 1-(K3A,K4A)-myc_c was specific to these residues rather than a general effect of changing overall charge of the N terminus.

We also examined the structural impact of mutating the patch of hydrophobic residues immediately downstream of Lys-3 and Lys-4, leucine (Leu-5), and valine (Val-6), which have also been implicated in functional coupling (12). As described above, the modeling (Fig. 5C) predicted a conformational rearrangement of the β 1-subunit upon mutation of Leu-5 to alanine

(β 1-L5A-myc_c) but not Val-6 to alanine (β 1-V6A-myc_c). Indeed, co-expression of the β 1-L5A-myc_c subunit resulted in a significantly attenuated left shift in $V_{0.5max}$ to only $-2.9 \pm 2.7 \text{ mV}$ ($n = 10$). This shift was intermediate between that of ZERO with β 1-myc_c and ZERO alone (Fig. 6, A, B, and C), indicating that the L5A mutation significantly inhibited, but did not totally abolish, the effects found with wild-type β 1-subunit on BK channels on $V_{0.5max}$. Moreover, with the β 1-L5A-myc_c subunit, BK channel activation and deactivation were still significantly slowed to 1.8 ± 0.1 and $5.9 \pm 0.9 \text{ ms}$, respectively ($n = 10$). These values were similar to the effect of wild-type β 1 (see Fig. 4, D and E). Mutation of the only other leucine residue in the N terminus, Leu-17, which we identified in our cell surface expression assays to be important for β 1-subunit-mediated trafficking of ZERO, to alanine had no effect on functional coupling. β 1-L17A-myc_c behaved similarly to wild-type β 1-myc_c subunit by left-shifting the G/V relationship to a $V_{0.5max}$ of $-26.3 \pm 3.1 \text{ mV}$ ($n = 10$). Again, as predicted by the structural modeling, mutation of Val-6 to alanine (β 1-V6A-myc_c) also resulted in a significant left shift in $V_{0.5max}$ (to $-29.7 \pm 5.6 \text{ mV}$, $n = 10$), comparable with that observed with wild-type β 1-myc_c. Taken together, these data reveal that distinct residues on the β 1-subunit N terminus control trafficking (membrane-proximal Leu-17) and functional coupling (membrane-distal Lys-3, Lys-4, and Leu-5), respectively.

Discussion

These data reveal that different residues on the short intracellular N terminus of β 1-subunits control trafficking and functional regulation of BK channel α -subunits. The membrane-

proximal amino acids of the β 1-subunit N terminus are important for the enhancement of BK α -subunit surface expression with Leu-17 playing an important role and residues distal to residue 14 being dispensable for this trafficking effect. In contrast, membrane-distal residues play a critical role in functional coupling with the basic lysine pair (Lys-3 and Lys-4) as well as the downstream hydrophobic leucine (Leu-5) having an important role.

β 1-subunits have been reported to exert diverse effects on BK channel α -subunit cell surface expression with both inhibition and enhancement of α -subunit surface expression reported. For example, an endocytic motif in the β 1-subunit C terminus has been reported to suppress cell surface expression of hSlo α -subunits, whereas the avian β 1-subunit enhances surface expression of the α -subunit (7, 8). This divergence of mechanism is likely a function of the α -subunit splice variant. β 1-subunits enhanced the surface expression of α -subunit splice variants with a C-terminal -DEC motif (7), whereas suppression of surface expression was undertaken using the QEERL C-terminal α -subunit variant (8). Moreover, assembly of β 1-subunits with α -subunits appears to be dynamic including via signaling-dependent control of β 1-subunit trafficking from rab11a-positive endosomes as well as assembly in the endoplasmic reticulum (24). In our system, using the ZERO α -subunit splice variant that includes the -DEC C-terminal motif, mammalian β 1-subunit enhanced the surface expression of the ZERO variant isoform more than 2-fold, a mechanism that is dependent on an intact N terminus of the β 1-subunit that, at least in part, determines the efficiency of α -subunit exit from the ER.

Importantly, the first 14 residues of the N terminus were dispensable for this enhancement of surface trafficking of α -subunits with leucine 17 being identified as the only critical residue in the most membrane-proximal residues of the N terminus. In the avian system in which the β 1-subunit has a predicted longer N terminus and only ~40% sequence conservation, the first 42 amino acids (encompassing the N terminus and TM1) were sufficient to promote surface trafficking of α -subunits (7). Intriguingly, a membrane-proximal leucine residue (at position 20 in avian β 1 and the corresponding Leu-17 in murine β 1) was also an important determinant of cell surface expression, suggesting a potential common mechanism (7). In a number of different proteins, N-terminal leucine residues can contribute to atypical dileucine-like sorting motifs (25). Although mutation of residues upstream of the important Leu-17 to alanine had no significant effect on the enhancement of α -subunit trafficking, whether Leu-17 is part of a trafficking motif or may play a more structural role, for example in controlling TM1 orientation in the plasma membrane, which may be important for ER exit as suggested for β 4-subunits (26), remains to be determined. Moreover, the L17A mutant, in contrast to deletion of the entire β 1 N terminus, had only a partial effect on α -subunit (or β 1-subunit itself) surface expression. Thus Leu-17 may also play an important role in post-ER mechanisms of α -subunit/ β 1-subunit sorting or assembly (24).

In contrast to the role of Leu-17 in trafficking, our data revealed that Leu-17 is not important for functional coupling. Although it has long been appreciated that the cytosolic N ter-

minus of the β 1-subunit is required for functional coupling with α -subunits (*e.g.* see Refs. 13 and 14), only relatively recently have specific residues in the β 1-subunit N terminus been defined as important contributors to functional coupling. For example, the basic residues Lys-3 and Lys-4 have been proposed to provide a specific mechanism to stabilize the voltage sensor of α -subunits such that when mutated to alanine gating charge movements were abolished (10) without affecting the conductance-voltage relationship in the absence of calcium. These data suggested that Lys-3 and Lys-4 interact with a cytosolic domain of the α -subunit. Moreover, Liu *et al.* (12) reported that both the adjacent hydrophobic motif of Leu-5, Val-6, and Met-7 and an electrostatic site formed by Glu-13 and Thr-14 interacted with the C terminus of α -subunit to control calcium sensitivity of BK channels. Indeed, independent biophysical and biochemical approaches suggest that the cytosolic domains of β 1-subunits must be close to the voltage-sensing domains of α -subunits (15, 16, 27). Furthermore, these data support that the transmembrane segments of β 1-subunits (TM1 and TM2) are spatially arranged close to the S0 transmembrane domain of α -subunits. Taken together, the membrane-distal residues of the β 1-subunit N terminus are likely to act as the key determinants of functional coupling of β 1-subunits with α -subunits. As both TM1 and TM2 of β 1-subunits are required for functional coupling (28), this would further suggest that the correct spatial organization of these transmembrane domains with the α -subunit is required for functional regulation.

Importantly, the predicted amphipathic helix on the N-terminal membrane-proximal domain of β 1-subunit may provide the structural basis for the important roles the basic Lys-3 and Lys-4 residues and the hydrophobic patch play in perhaps controlling the correct spatial orientation of the β 1-subunit within the α -subunit complex. Whether this involves interaction with multiple domains of the α -subunit or providing a β 1-subunit-dependent interface between the plasma membrane and α -subunit remains to be determined.

Intriguingly, the specific residues involved in β 1-subunit-dependent trafficking and functional coupling with α -subunits are also largely distinct from N-terminal residues of β 1-subunit that are involved in regulation by other molecules such as ω -3 fatty acids (17). However, in the case of ω -3 fatty acids, potential interactions between Arg-15 and Cys-18 in the most membrane-proximal domain of the N terminus are important, suggesting that functional integrity of the same membrane-proximal domain required for efficient trafficking is important. Interestingly, recent reports have indicated somatic mutations in cancer alter both Lys-4 and Leu-5 residues (19, 20), and changes in BK channel activity have been linked to cancer cell proliferation and migration (21–23). However, whether mutation of Lys-4 and/or Leu-5 is involved in regulating native BK channel activity, cancer growth, or migration in tissues expressing β 1-subunits is not known.

Clearly, investigation of whether mutations of N-terminal β 1-subunits residues are observed in other diseases or of signaling molecules that differentially regulate BK channel function by targeting domains of the β 1 will be of interest. Finally, convergence of multiple mechanisms to control BK

β 1-subunit N terminus controls function of BK channels

channel properties, function, and regulation on the short intracellular N terminus of β 1-subunits further supports the role of β 1-subunits in specifying cell-specific function and behaviors.

Experimental procedures

Expression constructs

Plasmids encoding the full-length BK channel α -subunit ZERO splice variant with either an N-terminal FLAG tag or both a FLAG- and a C-terminal HA (-HA) tag were described previously (26).

A sticky-end PCR cloning strategy was adopted to generate -myc_c-tagged β 1-subunit constructs in the pcDNA3.1 vector. The human β 1-subunit was first amplified from a construct (a generous gift from Dr. Jon Lippiat, University of Leeds; Ref. 29) using primers NheI- β 1 fwd (5'-ACTCAGATCTGCTAGCATGGTGAAGAAG) and β 1-myc-XhoI rev (5'-ACTCGAGCTAAGATCCTCTTCTGAGATGAGTTTTTGTTCCTTCTGGGCCG). To make a construct with both extracellular and C-terminal myc tags (myc_{c&e}), site-directed mutagenesis with primers 5'-AGCCAAATTCCAAGAGCAGAACTCATCTCAGAAGAGGATCTTCAGG (fwd) and 5'-AAGCAGTAGAAGACCTGAAGATCCTCTTCTGAGATGAGTTCTGTC (rev) were used to introduce this additional myc_e tag between Gln-131 and Gln-132 of β 1-subunit. These two constructs then served as the templates to generate additional constructs with mutated intracellular N termini using either the KOD mutagenesis kit (Novagen) or PCR subcloning of amplicons with NheI and XhoI restriction tails. Primers used for the mutagenesis were as follows: β 1- Δ 6: fwd, 5'-AAGCTGGCTAGCCACGGTGAAGAAGCTG, and BGH rev (Life Technologies); β 1- Δ 17: fwd, 5'-AGCTGGCTAGCCAACATGCTGGGTGTAACCATGG, and BGH rev; β 1-(K3,4A): fwd, 5'-AGATCTACATGGTGGCGGCGCTGGTGATGGCCAGAAG, and rev, 5'-TCTGGGCCATCACCAGCGCCGCCACCATGTAGATCTGAG; β 1-L5A: fwd, 5'-TACATGGTGAAGAAGCGGTGATGGCCAGAAG, and rev, 5'-TCTGGGCCATCACCGCTTCTTACCATGTAG; β 1-V6A: fwd, 5'-ATGGTGAGAAGCTGGCGATGGCCAGAAGCG, and rev, 5'-GCTTCTGGGCCATCGCCAGCTTCTTACCATG; β 1-(K10A,R11A): fwd, 5'-TGGTGATGGCCAGGCAGCAGGAGAGACACGAG, and rev, 5'-TCGTGTCTCTCCTGCTGCCTGGGCCATCACCAG; β 1-(R11A,G12A,E13A): fwd, 5'-TGGTGATGGCCAGAAGGCGGCAGCGACACGAGCCCTTTGCC, and rev, 5'-AGGCAAAGGGCTCGTGTCTGCTGCCGCTTCTGGCCATCACC; β 1-T14A: fwd, 5'-AGAAGCGGGAGAGACACGAGCCCTTTGCC, and rev, 5'-AGGCAAAGGGCTCGTGTCTCTCCCCGCTTCTG; β 1-R15A: fwd, 5'-AGAAGCGGGAGAGACACGAGCCCTTTGCC, and rev, 5'-AGGCAAAGGGCTCGTGTCTCTCCCCGCTTCTG; β 1-L17A: fwd, 5'-AGAGACACGAGCCGCTTGCTGGGTGTAACC, and rev, 5'-TACACCCAGGCAAGCGGCTCGTGTCTCTCC; and β 1-C18A: fwd, 5'-AGAGACACGAGCCCTTGCCCTGGGTGTAACCATG, and rev, 5'-ATGGTTACACCCAGGGCAAGGGCTCGTGTCTCTC-3'. All constructs were verified by sequencing.

Cell culture, transfection, and imaging

HEK293 cells were cultured and transfected with Lipofectamine 2000 according to a previously published protocol (26). Quantitative cell surface labeling of N-terminal FLAG epitope-tagged BK channel α -subunits in non-permeabilized cells was performed using mouse monoclonal anti-FLAG M2 antibody (Sigma) and secondary anti-mouse Alexa Fluor 543 (Invitrogen) at a dilution ratio of 1:100 and 1:1000, respectively. Cells were then fixed in 4% paraformaldehyde for 30 min, permeabilized with 3% Triton X-100 for 10 min, and blocked with phosphate-buffered saline containing 3% bovine serum albumin plus 0.05% Tween 20 for 1 h. For total BK channel expression, either the intracellular C-terminal HA epitope tag was probed with anti-HA polyclonal rabbit antibody (Zymed Laboratories Inc.; 1:500) followed by Alexa Fluor 647 (Molecular Probes; 1:1000), or the FLAG tag was probed with anti-FLAG antibody with anti-mouse Alexa Fluor 488 (1:1000).

Quantitative membrane expression of β 1-subunits with both myc_c and myc_e tags was detected using rabbit anti-myc (Immune Systems) at 1:300 and anti-rabbit secondary antibody conjugated to Alexa Fluor 546 prior to fixation and permeabilization. Total expression of β 1-subunits was probed with rabbit anti-myc antibody (Immune Systems) at 1:1000 and anti-rabbit secondary antibody conjugated to Alexa Fluor 488 at 1:1000. Co-expression of α - and β 1-subunits was determined as above with the exception that the anti-rabbit secondary antibody was conjugated to Alexa Fluor 647. Cells were mounted in Mowiol and dried at room temperature overnight in the dark before image acquisition.

Confocal images were acquired on a Zeiss LSM510 laser-scanning microscope using a 63 \times oil Plan Achromat (numerical aperture, 1.4) objective lens at Nyquist sampling rates in multitracking mode to minimize channel cross-talk. 3D image stacks were deconvolved using the program Huygens (Scientific Volume Imaging), and cell surface expression of full-length channels was determined by quantitative immunofluorescence calculated as the surface (FLAG-) to total channel protein (-HA or intracellular FLAG-) ratio using ImageJ (National Institutes of Health). For each cell, the absolute mean FLAG- and -HA immunofluorescence signal was determined following background subtraction in each channel. The absolute FLAG- to -HA ratio was then calculated and normalized to the ratio determined for the respective control as indicated in each figure that was run in parallel in each experiment. In each independent transfection (N), multiple cells were randomly selected, and an experiment average was determined for each construct. For statistical analysis, the average ratio in each independent experiment was used to calculate each group mean.

Colocalization of the different mutant β 1-subunits with the ER was assayed by co-transfecting the subunits with pDsRed-ER expressing the ER marker (Clontech). Confocal images were acquired and deconvolved as above, and Pearson's correlation coefficient (R) was determined using ImageJ with an R value of +1 indicating 100% colocalization.

Electrophysiology

Macropatch recordings were performed using the inside-out patch clamp configuration at room temperature essentially as described previously (30). Briefly, the extracellular recording solution was composed of 140 mM KMeSO₃, 2 mM KCl, 20 mM HEPES, 2 mM MgCl₂, pH 7.3. Internal solution was composed of 140 mM KMeSO₃, 2 mM KCl, 20 mM HEPES, 5 mM HEDTA, pH 7.3, with CaCl₂ added to give a free Ca²⁺ concentration of 10 μM. Voltage protocols and acquisition were controlled using an Axopatch 200B amplifier and Digidata 1440 using pCLAMP10. *G/V* relationships were constructed from tail currents recorded using a holding potential of −120 mV with 100-ms steps over a voltage range of −100 to +120 mV in 20-mV steps followed by a step back to −80 mV. *V*_{0.5max} was determined from Boltzmann fits of the normalized *G/V* curves using the following equation.

$$G/G_{\max} = 1/(1 + \exp(-ze(V - V_{0.5\max})/kT))$$

where *z* is the number of equivalent gating charges, *V*_{0.5max} is the voltage for half-activation of the channel, *e* is the elementary charge, *k* is the Boltzmann constant, and *T* is the absolute temperature. Activation and deactivation time constants were determined by fitting activation and deactivation curves to an exponential function.

Statistical analysis

All data are presented as means ± S.E. with *N* representing the number of independent imaging experiments or cells in electrophysiology assays and *n* representing the number of individual cells analyzed in imaging assays. Data from independent cells in electrophysiology experiments or independent experiments in imaging assays (*N*) were analyzed by ANOVA with post hoc Dunnett's test having significance set as follows: *, *p* < 0.05; **, *p* < 0.01; and ***, *p* < 0.001.

In silico structural analysis

Secondary structure of the wild-type β 1-subunit was predicted by submitting its protein sequence to the JPred online tool (31). Amphipathicity and potential helical secondary structure on the N-terminal region was analyzed with Heliquest (32). The initial tertiary structure of the first 50 N-terminal residues of the wild-type β 1-subunit was modeled using the I-Tasser web server (33). A number of probable models were built by the server based on multiple threading alignments followed by iterative assemblies of template fragments. The structure with the highest confidence score was next chosen to be further refined using the Swiss-PdbViewer Version 4.1 (34). Briefly, the last 10 residues of the modeled peptide were first trimmed to better reflect the predicted and reported consensus secondary structure before several rounds of side-chain fixations and energy minimization were applied sequentially until no further improvement could be achieved. Quality of the enhanced structure was assessed on both the WHAT-IF (35) and SWISS-MODEL structural assessment (36) web servers. This predicted wild-type model was then used as a template in the homology modeling of the mutated N-terminal β 1 peptides using the Multiple Mapping Method (MMM) web server (37). MMM

combines the best alternatively aligned fragments along the peptide into a final alignment used for the model construction. All the predicted mutant models were further refined and assessed as above. The rotational and translational orientation of each of the modeled peptide with respect to membrane lipid bilayers was next calculated using the PPM web server (38). The peptide/membrane molecular system was subsequently assembled with the lipid replacement method, equilibrated, and minimal dynamics-simulated in a synthetic environment of 1-palmitoyl-2-oleoyl-*sn*-glycero-3-phosphocholine lipid bilayers using the CHARMM-GUI web server (39). The 3D models were visualized using the program Chimera (40).

Author contributions—M. J. S. conceived and designed the study with L. C. M. J. S. coordinated and, with L. C., wrote the manuscript. L. C. generated constructs and performed and analyzed imaging and biochemical assays. D. B. performed and analyzed electrophysiological experiments. Z. H. L. performed the *in silico* modeling and provided the bioinformatics discussion. H. M. generated constructs and analyzed and produced data in Fig. 1. All authors reviewed the results, edited drafts, and approved the final version of the manuscript.

Acknowledgment—We are grateful to the IMPACT imaging facility in the Centre for Integrative Physiology for assistance in confocal imaging.

References

- Contreras, G. F., Castillo, K., Enrique, N., Carrasquel-Ursulaez, W., Castillo, J. P., Milesi, V., Neely, A., Alvarez, O., Ferreira, G., González, C., and Latorre, R. (2013) A BK (Slo1) channel journey from molecule to physiology. *Channels* **7**, 442–458
- Latorre, R., Castillo, K., Carrasquel-Ursulaez, W., Sepulveda, R. V., Gonzalez-Nilo, F., Gonzalez, C., and Alvarez, O. (2017) Molecular determinants of BK channel functional diversity and functioning. *Physiol. Rev.* **97**, 39–87
- Shipston, M. J., and Tian, L. (2016) Posttranscriptional and posttranslational regulation of BK channels. *Int. Rev. Neurobiol.* **128**, 91–126
- Sun, X., Zaydman, M. A., and Cui, J. (2012) Regulation of voltage-activated K⁺ channel gating by transmembrane β subunits. *Front. Pharmacol.* **3**, 63
- Zhang, J., and Yan, J. (2014) Regulation of BK channels by auxiliary γ subunits. *Front. Physiol.* **5**, 401
- Morrow, J. P., Zakharov, S. I., Liu, G., Yang, L., Sok, A. J., and Marx, S. O. (2006) Defining the BK channel domains required for β 1-subunit modulation. *Proc. Natl. Acad. Sci. U.S.A.* **103**, 5096–5101
- Kim, E. Y., Zou, S., Ridgway, L. D., and Dryer, S. E. (2007) β 1-subunits increase surface expression of a large-conductance Ca²⁺-activated K⁺ channel isoform. *J. Neurophysiol.* **97**, 3508–3516
- Toro, B., Cox, N., Wilson, R. J., Garrido-Sanabria, E., Stefani, E., Toro, L., and Zarei, M. M. (2006) KCNMB1 regulates surface expression of a voltage and Ca²⁺-activated K⁺ channel via endocytic trafficking signals. *Neuroscience* **142**, 661–669
- Dworetzky, S. I., Boissard, C. G., Lum-Ragan, J. T., McKay, M. C., Post-Munson, D. J., Trojnecki, J. T., Chang, C. P., and Gribkoff, V. K. (1996) Phenotypic alteration of a human BK (hSlo) channel by hSlo β subunit coexpression: changes in blocker sensitivity, activation/relaxation and inactivation kinetics, and protein kinase A modulation. *J. Neurosci.* **16**, 4543–4550
- Castillo, K., Contreras, G. F., Pupo, A., Torres, Y. P., Neely, A., González, C., and Latorre, R. (2015) Molecular mechanism underlying β 1 regulation in voltage- and calcium-activated potassium (BK) channels. *Proc. Natl. Acad. Sci. U.S.A.* **112**, 4809–4814
- Torres, Y. P., Granados, S. T., and Latorre, R. (2014) Pharmacological consequences of the coexpression of BK channel α and auxiliary β subunits. *Front. Physiol.* **5**, 383

β 1-subunit N terminus controls function of BK channels

- Liu, H.-W., Hou, P.-P., Guo, X.-Y., Zhao, Z.-W., Hu, B., Li, X., Wang, L.-Y., Ding, J. P., and Wang, S. (2014) Structural basis for calcium and magnesium regulation of a large conductance calcium-activated potassium channel with β 1 subunits. *J. Biol. Chem.* **289**, 16914–16923
- Orio, P., Torres, Y., Rojas, P., Carvacho, I., Garcia, M. L., Toro, L., Valverde, M. A., and Latorre, R. (2006) Structural determinants for functional coupling between the β and α subunits in the Ca^{2+} -activated K^+ (BK) channel. *J. Gen. Physiol.* **127**, 191–204
- Wang, B., and Brenner, R. (2006) An S6 mutation in BK channels reveals β 1 subunit effects on intrinsic and voltage-dependent gating. *J. Gen. Physiol.* **128**, 731–744
- Castillo, J. P., Sánchez-Rodríguez, J. E., Hyde, H. C., Zaelzer, C. A., Aguayo, D., Sepúlveda, R. V., Luk, L. Y., Kent, S. B., Gonzalez-Nilo, F. D., Bezanilla, F., and Latorre, R. (2016) β 1-subunit-induced structural rearrangements of the Ca^{2+} - and voltage-activated K^+ (BK) channel. *Proc. Natl. Acad. Sci. U.S.A.* **113**, E3231–E3239
- Liu, G., Zakharov, S. I., Yao, Y., Marx, S. O., and Karlin, A. (2015) Positions of the cytoplasmic end of BK α S0 helix relative to S1-S6 and of β 1 TM1 and TM2 relative to S0-S6. *J. Gen. Physiol.* **145**, 185–199
- Hoshi, T., Tian, Y., Xu, R., Heinemann, S. H., and Hou, S. (2013) Mechanism of the modulation of BK potassium channel complexes with different auxiliary subunit compositions by the ω -3 fatty acid DHA. *Proc. Natl. Acad. Sci. U.S.A.* **110**, 4822–4827
- Hoshi, T., Wissuwa, B., Tian, Y., Tajima, N., Xu, R., Bauer, M., Heinemann, S. H., and Hou, S. (2013) ω -3 fatty acids lower blood pressure by directly activating large-conductance Ca^{2+} -dependent K^+ channels. *Proc. Natl. Acad. Sci. U.S.A.* **110**, 4816–4821
- Seshagiri, S., Stawiski, E. W., Durinck, S., Modrusan, Z., Storm, E. E., Conboy, C. B., Chaudhuri, S., Guan, Y., Janakiraman, V., Jaiswal, B. S., Guillory, J., Ha, C., Dijkgraaf, G. J., Stinson, J., Gnad, F., et al. (2012) Recurrent R-spondin fusions in colon cancer. *Nature* **488**, 660–664
- Schulze, K., Imbeaud, S., Letouzé, E., Alexandrov, L. B., Calderaro, J., Rebouissou, S., Couchy, G., Meiller, C., Shinde, J., Soysouvanh, F., Calatayud, A.-L., Pinyol, R., Pelletier, L., Balabaud, C., Laurent, A., et al. (2015) Exome sequencing of hepatocellular carcinomas identifies new mutational signatures and potential therapeutic targets. *Nat. Genet.* **47**, 505–511
- Ge, L., Hoa, N. T., Wilson, Z., Arismendi-Morillo, G., Kong, X.-T., Tajhya, R. B., Beeton, C., and Jadus, M. R. (2014) Big Potassium (BK) ion channels in biology, disease and possible targets for cancer immunotherapy. *Int. Immunopharmacol.* **22**, 427–443
- Steinle, M., Palme, D., Misovic, M., Rudner, J., Dittmann, K., Lukowski, R., Ruth, P., and Huber, S. M. (2011) Ionizing radiation induces migration of glioblastoma cells by activating BK K^+ channels. *Radiother. Oncol.* **101**, 122–126
- Oeggerli, M., Tian, Y., Ruiz, C., Wijker, B., Sauter, G., Obermann, E., Güth, U., Zlobec, I., Sausbier, M., Kunzelmann, K., and Bubendorf, L. (2012) Role of KCNMA1 in breast cancer. *PLoS One* **7**, e41664
- Leo, M. D., Bannister, J. P., Narayanan, D., Nair, A., Grubbs, J. E., Gabrick, K. S., Boop, F. A., and Jaggar, J. H. (2014) Dynamic regulation of β 1 subunit trafficking controls vascular contractility. *Proc. Natl. Acad. Sci. U.S.A.* **111**, 2361–2366
- Foss, S. M., Li, H., Santos, M. S., Edwards, R. H., and Voglmaier, S. M. (2013) Multiple dileucine-like motifs direct VGLUT1 trafficking. *J. Neurosci.* **33**, 10647–10660
- Chen, L., Bi, D., Tian, L., McClafferty, H., Steeb, F., Ruth, P., Knaus, H.-G., and Shipston, M. J. (2013) Palmitoylation of the β 4-subunit regulates surface expression of large conductance calcium-activated potassium channel splice variants. *J. Biol. Chem.* **288**, 13136–13144
- Sun, X., Shi, J., Delaloye, K., Yang, X., Yang, H., Zhang, G., and Cui, J. (2013) The Interface between membrane-spanning and cytosolic domains in Ca^{2+} -dependent K^+ channels is involved in β subunit modulation of gating. *J. Neurosci.* **33**, 11253–11261
- Kuntamallappanavar, G., Toro, L., and Dopico, A. M. (2014) Both transmembrane domains of BK β 1 subunits are essential to confer the normal phenotype of β 1-containing BK channels. *PLoS One* **9**, e109306
- Lippiat, J. D., Standen, N. B., Harrow, I. D., Phillips, S. C., and Davies, N. W. (2003) Properties of BK(Ca) channels formed by bicistronic expression of hSlo α and β 1–4 subunits in HEK293 cells. *J. Membr. Biol.* **192**, 141–148
- Jeffries, O., Tian, L., McClafferty, H., and Shipston, M. J. (2012) An electrostatic switch controls palmitoylation of the large conductance voltage- and calcium-activated potassium (BK) channel. *J. Biol. Chem.* **287**, 1468–1477
- Cole, C., Barber, J. D., and Barton, G. J. (2008) The Jpred 3 secondary structure prediction server. *Nucleic Acids Res.* **36**, W197–W201
- Gautier, R., Douguet, D., Antonny, B., and Drin, G. (2008) HELIQUEST: a web server to screen sequences with specific α -helical properties. *Bioinformatics* **24**, 2101–2102
- Zhang, Y. (2008) I-TASSER server for protein 3D structure prediction. *BMC Bioinformatics* **9**, 40
- Guex, N., and Peitsch, M. C. (1997) SWISS-MODEL and the Swiss-PdbViewer: an environment for comparative protein modeling. *Electrophoresis* **18**, 2714–2723
- Hekkelman, M. L., Te Beek, T. A., Pettifer, S. R., Thorne, D., Attwood, T. K., and Vriend, G. (2010) WIWS: a protein structure bioinformatics Web service collection. *Nucleic Acids Res.* **38**, W719–W723
- Kiefer, F., Arnold, K., Künzli, M., Bordoli, L., and Schwede, T. (2009) The SWISS-MODEL Repository and associated resources. *Nucleic Acids Res.* **37**, D387–D392
- Rai, B. K., and Fiser, A. (2006) Multiple mapping method: a novel approach to the sequence-to-structure alignment problem in comparative protein structure modeling. *Proteins* **63**, 644–661
- Lomize, M. A., Pogozheva, I. D., Joo, H., Mosberg, H. I., and Lomize, A. L. (2012) OPM database and PPM web server: resources for positioning of proteins in membranes. *Nucleic Acids Res.* **40**, D370–D376
- Wu, E. L., Cheng, X., Jo, S., Rui, H., Song, K. C., Dávila-Contreras, E. M., Qi, Y., Lee, J., Monje-Galvan, V., Venable, R. M., Klauda, J. B., and Im, W. (2014) CHARMM-GUI Membrane Builder toward realistic biological membrane simulations. *J. Comput. Chem.* **35**, 1997–2004
- Pettersen, E. F., Goddard, T. D., Huang, C. C., Couch, G. S., Greenblatt, D. M., Meng, E. C., and Ferrin, T. E. (2004) UCSF Chimera—a visualization system for exploratory research and analysis. *J. Comput. Chem.* **25**, 1605–1612